Inertia Reduction using Interaction Control Approach for Mecanum Wheeled Vehicle on Cornering Road

Norsharimie Mat Adam [1], Addie Irawan [2*]

[1] Automotive Engineering Centre (AEC), Universiti Malaysia Pahang, 26600 Pekan, Pahang, Malaysia
[2] Robotics, Intelligent Systems & Control Engineering (RISC) Research Group, Faculty of Electrical & Electronics Engineering Technology, Universiti Malaysia Pahang, 26600 Pekan, Pahang, Malaysia
[1] sharimie.adam@gmail.com; [2] addieirawan@ump.edu.my
* Corresponding Author

ARTICLE INFO

ABSTRACT

The paper presents a dynamic control approach using impedance control to reduce inertia factors acting on a Mecanum Wheeled Vehicle (MWV) on cornering roads. Inertia in a mobile vehicle is one of the issues that affect the safety and energy efficiencies of the vehicle, especially when maneuvering on cornering and confined paths. With reference to the problem statements in the dynamics analyses, velocity-based impedance control was proposed where the derived interaction translational forces on the vehicle that consider friction and touching forces on vehicle-terrain are controlled through the velocities of the vehicle. This study emphasized shaping the axial velocities input of the MWV for both longitudinal and latitude motions to control the sensitivity of the vehicle during cornering periods. The verification was done through several simulations on the proposed velocity-based impedance control on the MWV plant. The results show that the different forces on MWV axial motion were capable of reducing inertia via velocity input during the cornering period of maneuvering by increasing the stiffness and damping ratio of the controller at about 2 and 9 for stiffness x-axis and y-axis, respectively, and 15 and 10 for damping ration of the x-axis and y-axis respectively. Moreover, with the proposed controller, inertia on MWV can be controlled on the slippery road such as asphalt roads. This scenario has influenced the overall kinetic energy of the vehicle down to about 26%, thus, able to control the overdriven occurred on cornering road.

1. Introduction

An omnidirectional wheeled vehicle (OWV) is configured with a fully actuated mechanism that requires a different perspective of control compared to the skid or steering-wheeled vehicle that is configured with an underactuated mechanism. This holonomic configuration is commonly designed for a wheeled mobile robot (WMR) that deploys omni-move normally on flat terrain. Major control system design works for this vehicle are towards better motion planning for stability maneuvering purposes other than precision in its autonomy function. According to Seigwart and Nourbakhsh, the speed of each Omni wheel, according to its orientation angle and the intended direction, can be mathematically derived for control system design [1]. This concept has been held by many researchers, such as Chang et al., in their works considered a mathematical method solution in controlling the

speed of each Omni wheel based on the vehicle orientation angle and direction [2]. The Omni-move characteristic on an Omni wheel can increase its flexibility up to two-dimensional motion wherever the vehicle is freely moved without depending on pitching control [3], such as in steering vehicles [4, 5]. As shown in Fig. 1, the mecanum wheel is an example of an Omni wheel that is commonly used for different duties of payload. The wheel consists of rollers around the surface body of the wheel depending on its size, and the mecanum's roller assembled in the b-axis is 45° skewed to the a-axis wheel [6]. The OWV is major used and applicable for the confined space in which need to neglect the operation where there is a need for the vehicle to turn by pitching some group or front wheels such as rack steering vehicle. However, inertia and overdriven still can be occurred in this type of vehicle due to the system still having a moving rigid body. With the applicability of confined space deployment, the incident such as collision with the wall or hit the road boarder is high possibility occurred.
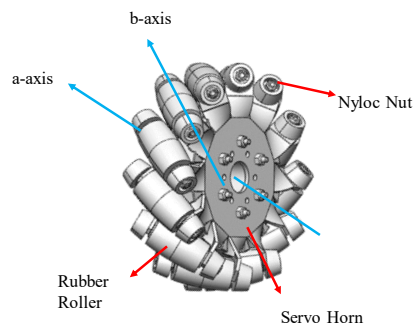

Fig. 1. Example of Omni wheel; mecannum wheel specification

Therefore, in this research, inertia and overdriven control are introduced through impedance control of the overall OWV during a maneuver on the cornering path. The velocity-based impedance control was proposed to cater to the speed and kinetic energy of the OWV whenever this vehicle reaches the cornering path. The contribution of this work is to provide an alternative control method by using the interaction control from the relationship between the wheel of the vehicle and the terrain of the road that is able to control the inertia of the vehicle indirectly.

2. Related Works

2.1. Inertia Issues on Omnidirectional Wheeled Vehicle/Robot

Several studies and works have approached the dynamic path motion with stable orientation, especially in the case of cornering, roundabout, and harsh roads. One of the issues that give impact the stability of wheeled vehicle/robot maneuvering is inertia. The inertia of the wheeled system is a vital element, yet it is usually difficult to be controlled [7]. Inertia happens due to overdriven during braking, wheel slipped, and sharp turning [8] by the vehicle, which may cause accidents and destruction to the vehicle system. On the other hand, inertia happened due to the wheel-slipped during cornering as well. Therefore, several approaches have been made by researchers to overcome this matter either through control approach, tactical sensing method, estimation solutions, or maybe hybrid method such as done in [9-11]. Fu and Hill, in their works, stabilized the omnidirectional robot by the proposed multi-stages control strategy that considered pod-angle and force-based wheel controller that is robust to the longitudinal wheel slip [12]. The wheels' slipping effects are a crucial problem for wheeled vehicle stability, and this incident appears commonly in practice. Therefore, Cui et al., in their works, introduced the unscented Kalman filter (UKF) with a low pass filter for real-time estimation of the slipping parameters and stable tracking control law using the backstepping method to tackle the vehicle constraints [13].

Slippery cases, on the other hand, can contribute to overdriven as well. It was noted that the terrain was slippery, which made the vehicle understeer [14]. Commonly, the standard vehicle system was unaware of the condition, making the driver continue to turn harder. At some point, the accident cannot be avoided since the vehicle has reached its minimum turning radius, and it is getting worse in the

case of a road with a cornering path. Here the estimation method became handy. For example, researchers in [15] had developed a real-time center of gravity (CoG) position estimator integrated with an adaptive Kalman filter-extended Kalman filter (AKF-EKF) [15] to reduce the overforce of the lightweight wheeled mobile robot through both front or rear torque on wheels. Xiao et al., on the other hand, have approached the model predictive control (MPC) to suppress the inertia of the wheeled vehicle through the tracking control of the motion path [16]. The same goes for Pinheiro et al., whereby MPC was approached to control the speed and consider the non-slipping constraint of the omnidirectional WMR to avoid slippages [17]. Other than the prediction method, robust control with a model-based approach has become one of the favorable solutions to the wheeled vehicle in a similar problem. For example, Deremetz et al. used the backstepping control approach to solve the balancing problem on the lateral effects of wheeled vehicles, notably the sideslip angles, and an observer was used to estimate the sliding [18]. This model reference approach permits feeding the proposed control laws appropriately, enabling an orientation keeping along the trajectory and guaranteeing the accuracy of its path tracking. For the specific OWV system, Adamov et al. proposed the solution by using the approach of multiplication of the velocity of each wheel by the cosine angle at the desired direction projected on each Omni wheel-driven direction [19]. Numerous efforts have gained the stability of a wheeled vehicle other than smoothest path motion whenever the vehicle faces a critical road, such as cornering and rough terrain [20-22]. As an underactuated vehicle system subjected to holonomic constraints, OWV tends to move its posture, such as spinning or turning during breaking at the cornering path [23]. For example, reported in [24], the efforts are focused on improving path planning by focusing on path tracking and accuracy with different control techniques. However, the friction that happens on the OWV is practically unbounded with the different workspace. The situation degrades the tracking control performances every time the friction change. The modification exceeds the permitted scope. As a result, the kinodynamic problem arises, which necessitates a solution for both kinematics and dynamics in order to optimize the current states dynamically [25].

One method that has the potential to be used to address wheeled vehicle usability issues is the dynamics control approach. This control strategy is not limited to explicit force control. According to Xiao et al., the torque of each wheel can be controlled using a least square algorithm. Here, the upper and lower controllers were developed, where torque for each wheel is controlled in the lower controller, resulting in a stable and efficient system during operation [26]. Other than torque control, impedance or admittance control also has the potential to be explored for vehicle stability control solutions. As reported in [27], fuzzy predictive control on impedance control was applied and showed effectiveness for unstructured environment problems as the instructions are verified. Moreover, Hori et al., in their works, have used impedance control for the high back drivability with driving force control in which external forces applied by human hands and driving forces are estimated by disturbance observer with some proposed assist control methods [28]. On the other hand, a hybrid method was proposed in [29] in which to cater to the pinion angle of the rack-mounted electric power steering control for both lateral and impedance control of an autonomous vehicle. Unlike explicit force control, this control considered both contact forces and the position state of the system in controlling the system behavior [30]. For example, deployed on Hexarotor vehicle as reported in [31] where the sensitivity of the vehicle is controlled by the impedance control derived from dynamics of the vehicle without any touching forces. There are apparent constraints on system operation and reaction speeds, which will reflect in the relationship. As a result, a control law must be developed to establish a relationship between the robot system and the environment. In order to assure the effectiveness and robustness of this interactive control on the targeted plant, a compliant approach is required. Optimal tune of all mass–spring–damper elements such inertia, viscosity/damper and; allowing compliance with the environment, depending on the task. However, because this approach is indirect, the environment must be known in order to precisely manage the contact forces. When unforeseen obstructions create major trajectory deviations, huge forces are generated that can be harmed by friction [32]. Other than adaptive physical interation like commonly deployed on robot system, this sort of dynamic control has the possibilities to be used for shaping the energy to control the wheel robot and inertia vehicles indirectly. As used in [31], force/torque distributions from the dynamics

model of the wheeled vehicle can be estimated using the Euler–Lagrange, wherein the control algorithms can be obtained.

2.2. Problem Statement

An OWV with mecanum wheels was chosen as a framework for this research because this configuration has become more popular in wheeled robot development, particularly in limited space transport. In addition, the research focuses on the vehicle's cornering phase, which is critical in dealing with friction and inertia in order to avoid collision in a limited space, as shown in Fig. 2.
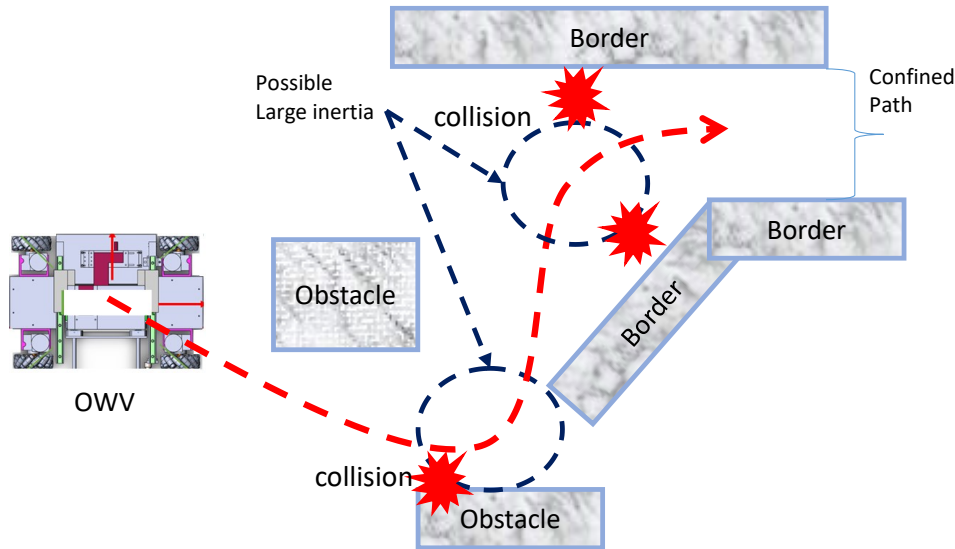

Fig. 2. An example of OWMR turning motion and inertia that may lead to a collision with a surrounding object

This issue's major concern is achieving the smoothest route motion [22], particularly in the area of the cornering point. As a fully actuated vehicle that is exposed to holonomic limitations, OWV with mecanum wheels exhibits body orientation changes, including minor spinning, throughout the breaking phase, particularly at cornering points, as seen in Fig. 2. Previously published research has shown that a vehicle's path planning performance can be improved using a variety of various control techniques [33-38]. In a real situation, the friction that happens on the holonomic vehicle is unpredictable or unbounded due to the variety of operating settings and terrain types. When the uncertain friction changes beyond the allowable range, these controls become inactive, resulting in poor tracking performance. This may contribute to the kinodynamics issue, which requires simultaneous resolution of kinematics and dynamics in order to receive reliable control input from the present state [25].

3. Interaction Control Design

According to the dynamic model of mecanum wheeled vehicle (MWV) [23], velocity-based impedance control is derived as interaction control for MWV according to the kinematics system expressed in (1) as follows [39]

$$
\begin{bmatrix} W_1 \\ W_2 \\ W_3 \\ W_4 \end{bmatrix} = \begin{bmatrix} 1 & 1 & l\,sin\left(\frac{\pi}{4}-\alpha\right) \\ 1 & -1 & l\,sin\left(\frac{\pi}{4}-\alpha\right) \\ -1 & -1 & l\,sin\left(\frac{\pi}{4}-\alpha\right) \\ -1 & 1 & l\,sin\left(\frac{\pi}{4}-\alpha\right) \end{bmatrix} \begin{bmatrix} cos\,\theta & sin\,\theta & 0 \\ -sin\,\theta & cos\,\theta & 0 \\ 0 & 0 & 1 \end{bmatrix} \begin{bmatrix} {}^gX_1 \\ {}^gY_1 \\ {}^g\theta \end{bmatrix}
\tag{1}
$$

where $q = [\overset{g}{X} \quad \overset{g}{Y} \quad \overset{g}{\theta}]^T$ are the cartesian of the MWV and, W_n are represented as the angular velocity of the MWV's wheels ($i = 1...4$). In MWV maneuvering, the only part that continuously contacts and interacts with the environment is its wheels. Any changes between wheels and environment interaction will affect the overall attitude and dynamics of the vehicle. According to this relationship, the interaction force between the vehicle wheels can be monitored and the affected motion to the vehicle's condition to maintain the stability of the vehicle system. Here, the elastic model between the vehicle body attitude and axial vehicle forces can be derived from the dynamics of MWV as illustrated in Fig. 3. The derived velocity-based impedance control is designed as a conjunction controller to the MWV speed control whereby the dynamic relationship between the velocity deviation and the axial forces from the dynamic changes of the torque on the wheel is regulated. Therefore, a velocity-based impedance control for MWV can be adopted as expressed in (2) as follows

$$F_v = M_f \Delta \ddot{q} + D_f \Delta \dot{q} + K_f \Delta q \tag{2}$$

where $F_v = [f_x \quad f_y \quad f_\theta]$ is indicated as Cartesian interaction forces of overall vehicle posture and $q \in \Re^3$ described the axial states of the vehicle in which $M_f(\ddot{q}) \in \Re^{nxm}$ represents the desired inertia matrix of the vehicle, $D_f(\dot{q}) \in \Re^{nxm}$ is the damping matrix of the vehicle and $K_f(q) \in \Re^n$ indicates the target stiffness of the vehicle system ($n = 3, m = 1$). Both D_f and K_f are in a diagonal form as expressed in (3), which specified for each Cartesian of the vehicle

$$D_f = diag(D_X \quad D_Y \quad D_\theta)$$
$$K_f = diag(K_X \quad K_Y \quad K_\theta) \tag{3}$$

On the other hand, the Cartesian interaction forces of MWV were derived from developed torques on each mecanum wheel (τ_i) [23] as can be expressed in (4) as follows

$$f_x = \sum_{i=1}^{4} (\tau_i - r \, sgn(\dot{W}_{o\,i}) f_i) \frac{\partial \overset{g}{W}_{o\,i}}{\partial \overset{g}{X}_1},$$
$$f_y = \sum_{i=1}^{4} \left(\tau_i - r \, sgn(\overset{g}{W}_{o\,i}) f_i \right) \frac{\partial \overset{g}{W}_{o\,i}}{\partial \overset{g}{Y}_1}, \tag{4}$$
$$f_\theta = \sum_{i=1}^{4} \left(\tau_i - r \, sgn(\overset{g}{W}_{o\,i}) f_i \right) \frac{\partial \dot{W}_{o\,i}}{\partial \overset{g}{\theta}}$$
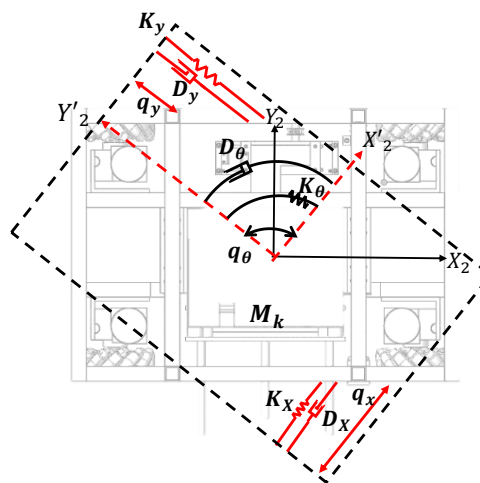

Fig. 3. Equivalent spring–mass–elastic damper model for MWV system posture.

The desired inertia, as shown in Fig. 3, is represented $M_f = diag(M_k)$ with $k = \{X, Y, \theta\}$. Moreover, D_k, K_k and M_k are the tuning parameters with $F_v \to 0$ and, both natural frequency (ω_0) and damping ratio (ζ_f) can be rearranged and expressed in (5) as follows, according to Newton's Second Law [40].

$$\omega_0 = \sqrt{\frac{K_k}{M_k}}, \zeta_f = \frac{D_k}{2\sqrt{M_k K_k}} \tag{5}$$

Therefore, the relationship between D_k, K_k and M_k can be expressed as in (6) using underdamped mode as follows

$$D_k = \zeta_k\, 2\sqrt{K_k M_k} \tag{6}$$

As a result, the control law for velocity shaping on MWV can be formulated as in (7) by integrating (5) to (2) as follows

$$v_{imp}(q) = \Delta\dot{q} = (K_k M_k)^{-\frac{1}{2}} \left(F_V - M_k \Delta\ddot{q} - K_k \Delta q\right) \tag{7}$$

The overall control system structure for MWV with proposed velocity-based impedance can be illustrated as shown in Fig. 4.
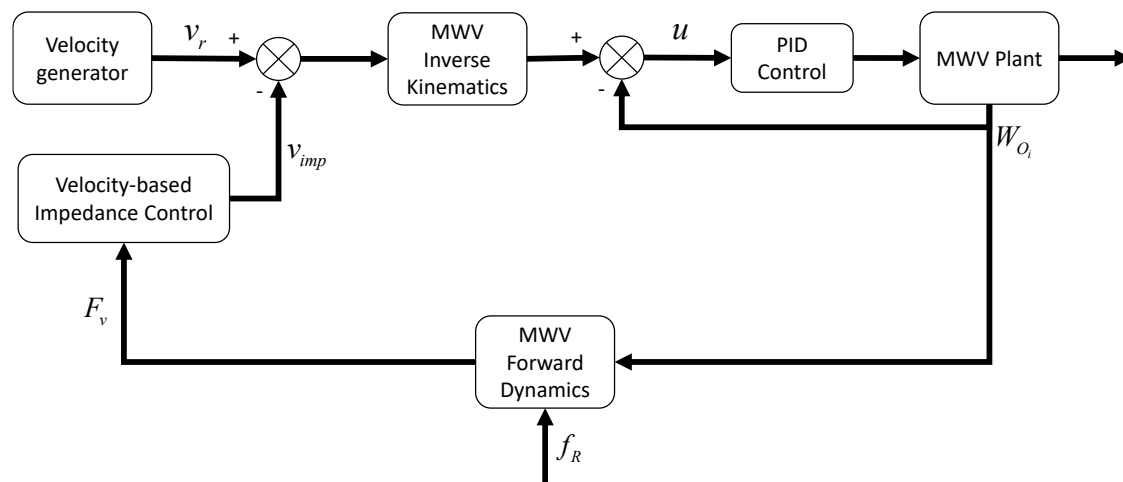

Fig. 4. Velocity-based impedance control system diagram for MWV

4. Results

The discussion and analysis of dynamic modeling are emphasized on the first, second, third, and fourth cornering of the samples motions as marked in Fig. 5. Between 1 sec and 263 secs of simulation time, the rotational velocity of each wheel performed in different values and poles. For the first cornering, the period was between 8 secs and 53 secs, the second cornering was 61–111 secs, the third cornering was 115–172 secs, and the fourth cornering was 175–226 secs.

4.1. Free Simulation Running without Interaction Control for Dynamic Observation and Analysis on MWV Model on Different Types of Terrain

As for the first step of verification works, the MWV model plant was tested with several running with only speed control (without impedance control) using the designed cornering path planning trajectory in order to observe and analyze its dynamic performances. According to these free running, the different performance of wheel angular velocity (W) performances with different interaction forces (F_v) can be depicted via different developed torque performances on each wheel, as shown in Fig. 6.
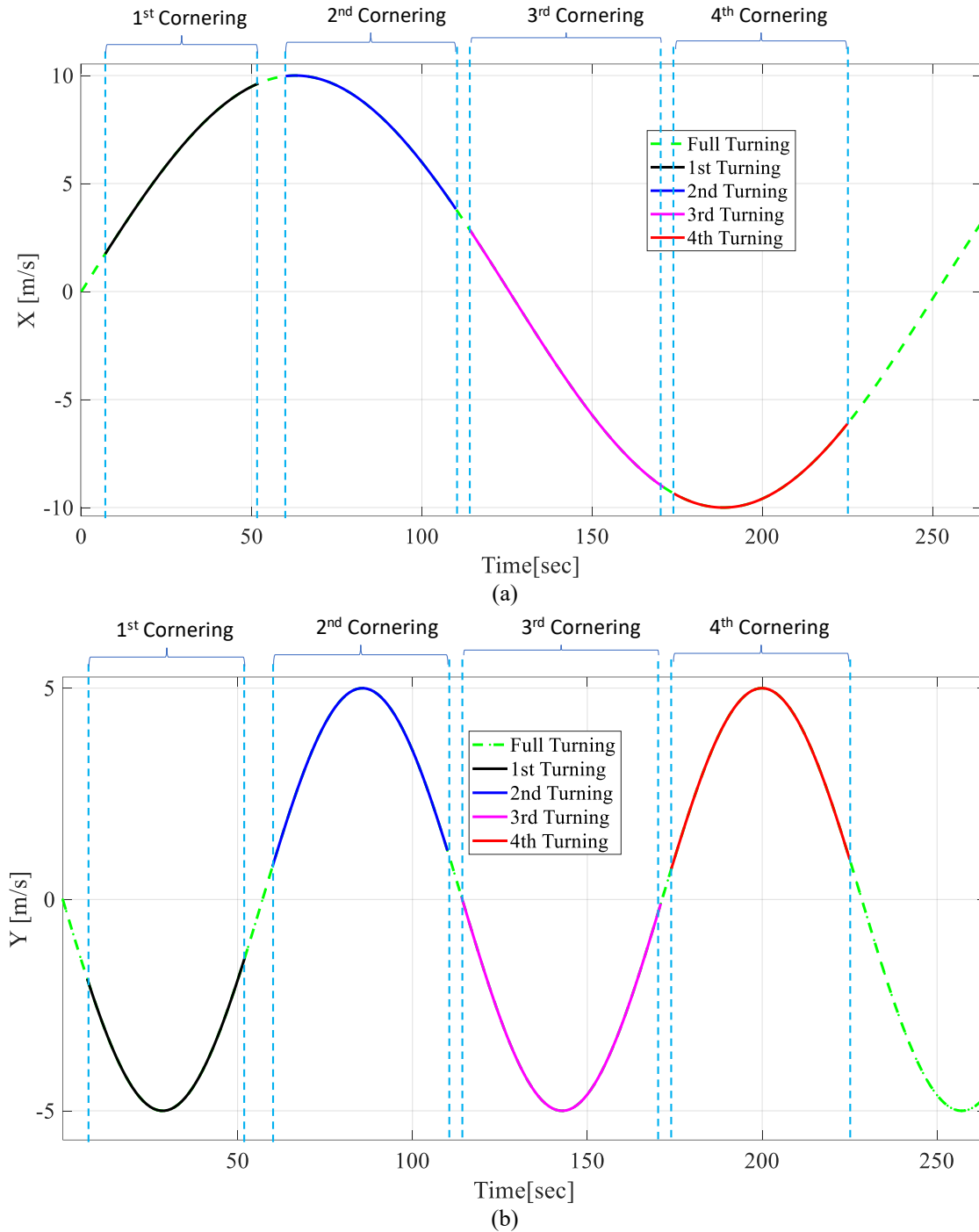
Fig. 5. Sample of cornering path planning velocity input for the simulation running on the MWV; (a) *X*-axis for cornering sample period, (b) *Y*-axis for cornering sample period

For example, in the first cornering, as shown in Fig. 6(a), the W_1 and W_2 velocities increased with different curves where τ_1 drastically decreased at 18 s and increased at the opposite poles with τ_2 as shown in Fig. 6(b). It is different to the W_3 and W_4 whereby these couple of wheels are gradually decelerated with almost mirroring the speed and torque performances of W_1 and W_2, respectively. The free running simulation also done on two different types of terrain as disturbances to the MWV with the different coefficients as tabulated in Table 1.

Table 1. List of different coefficients for different terrain

Terrain	Coefficient of static friction (μ_s) (type of mecanum wheel)	Coefficient of kinetic friction (μ_k)
Asphalt (concrete)	1	0.93
Earth road	1	0.55

(a)

(b)
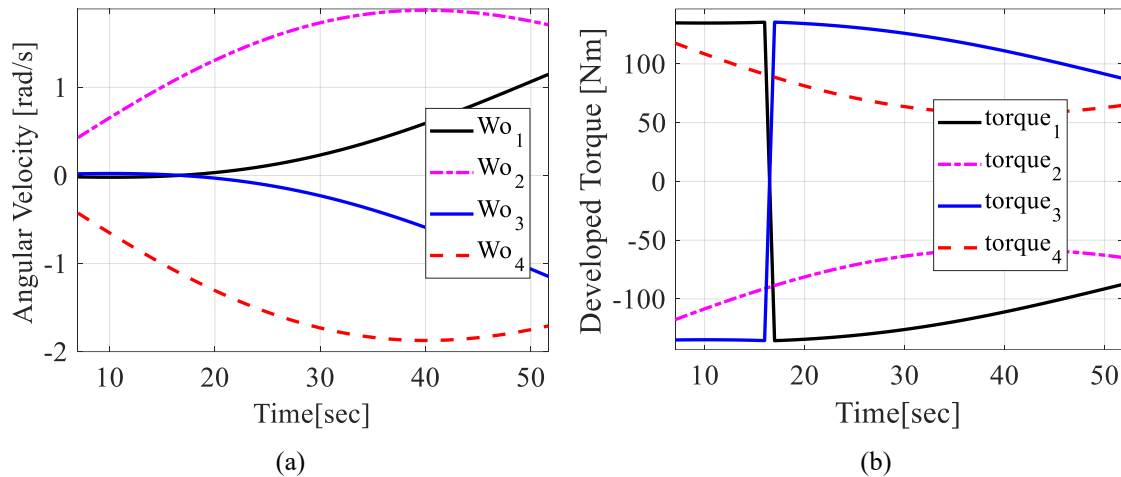
Fig. 6. A sample performance of the first cornering MWV (a) sample of angular velocity result for each wheel (b) sample of torque result for each wheel

The free running simulation on these different types of terrain also shows different interaction force results for different types of terrain. For example, in the second cornering motion, as shown in Fig. 7, MWV that runs with the asphalt (concrete) terrain shows f_x vector at about 2.7 N was applied at the longitudinal as compared to the MWV on the earth road with only about 2.2N. The same goes for the latitude forces f_y whereby MWV on the asphalt terrain is about 4.3 N which is 0.5N bigger than MWV on the earth road. A similar range pattern can be depicted in Fig. 8, whereby the major energy was applied to MWV crossing the asphalt type of road as compared to earth. These can be seen on each cornering path. For example, in the last cornering, as shown in Fig. 8, the kinetic energy used by MWV on earth road was fewer than maneuvering on asphalt road at about 77.2 J. Table 2 shows the summary of the MWV dynamics performance for this free simulation running.

Table 2. The overall performance between interaction forces and kinetic energy

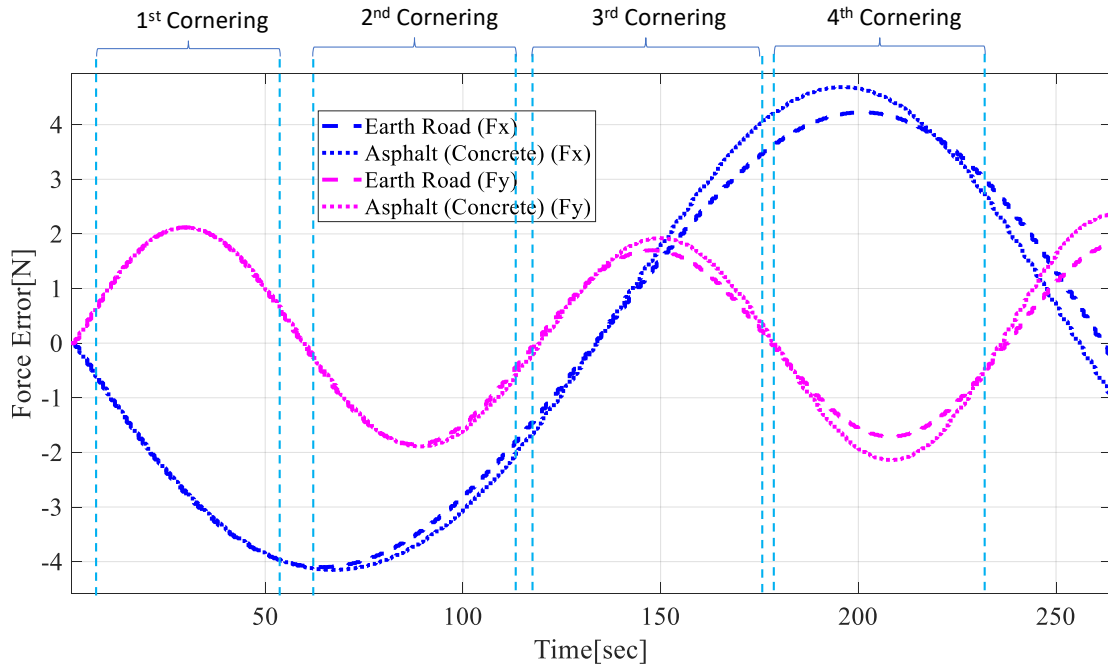| Terrain	Parameters	Cornering			
		1st	2nd	3rd	4th
Asphalt (concrete)	Cornering Angles	134°	55°	145°	40°
	W	1.35 m/s	1.48 m/s	1.25 m/s	1.58 m/s
	Average energy	25.6 J	31.2 J	23.1 J	32.5 J
	F_v	$f_x < f_y$	$f_x < f_y$	$f_x > f_y$	$f_x > f_y$
Earth road	Cornering Angles	134°	55°	145°	40°
	W	1.25 m/s	1.38 m/s	1.15 m/s	1.48 m/s
	Average energy	24.8 J	30.1 J	22.3 J	30.2 J
	F_v	$f_x < f_y$	$f_x < f_y$	$f_x > f_y$	$f_x > f_y$

Fig. 7. Sample of interaction forces (f_x, f_y) performances when MWV simulated on different types of terrain
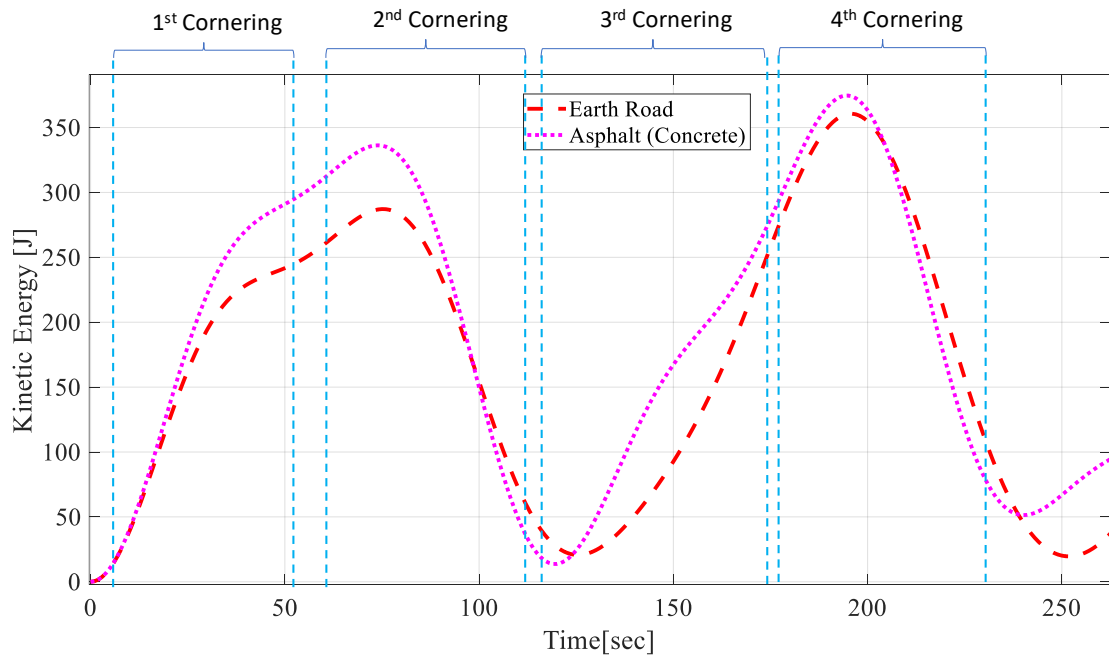

Fig. 8. Sample of kinetic energy performances when MWV simulated on different types of terrain

4.2. Analysis of Velocity-Based Impedance Control on MWV at Different Cornering Paths for Different Tuning

According to Section A, the analysis shows that asphalt road contributes more slippery than earth roads. The more slippery the terrain, the more inertia will be developed. Therefore, in verifying the proposed dynamic controller, the simulation was done and divided into three different tuning values for both K_X and K_Y in three different simulation sessions notified as T_1, T_2, and T_3 respectively, shown in Table 3. In addition to the first simulation, $K_X = K_Y = 1$ was depicted and ζ for each axis showed different results for different axials, as shown in Fig. 9 and Fig. 10.

Table 3. Fine-tunned stiffness and damping ratio values for each session of simulation

Simulation session	Stiffness (Nm^{-1})		damping ratio (ζ)	
	K_X	K_Y	ζ_X	ζ_Y
T_1	1	1	1	1
T_2	2	6	9	4
T_3	2	9	15	10

As shown in Fig. 9 and Fig. 10, the result of the ζ affected the shape of the velocity input of the OWV for both axial, respectively. As shown in Fig. 9, whenever K_X was increased the horizontal of vehicle (x-axis) getting slower approximately by 0.02 m/s for T_2 and 0.15 m/s for T_3. As shown in Fig. 10, the similar situation happened in which the vehicle getting slower at about 0.08 m/s in T_2 and 0.17 m/s in T_3. According to these results, MWV took the concentration on its axle weight as centroid and began spinning. In other words, OWV performs speed and rotational behavior due to its weight concentration. Moreover, whenever the mass shifts near the frontal axle, the MWV moves forward and vice versa.

There is an interaction between the location of the center of mass and the direction of the driving force. This interaction shows affect the direction of the translation of the vehicle and rapidly changes direction, as can be seen in every each cornering path as shown in Fig. 11. All these are affected by the inertia performances that can be measured through the kinetic energy as shown in Fig. 12. The energy reduced to approximately 18% for T_2 and 26% for T_3 whenever the stiffness and damping ratio were increased. These are due to the shaping of velocity input that can be depicted through the velocity input performances of the MWV, as shown in Fig. 13.
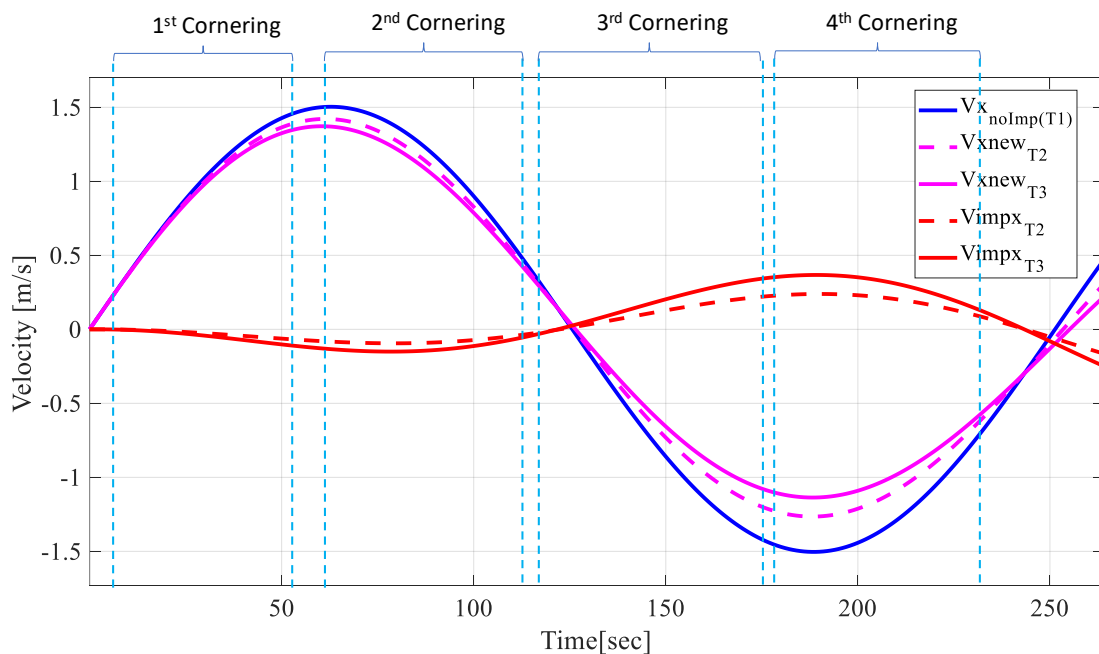
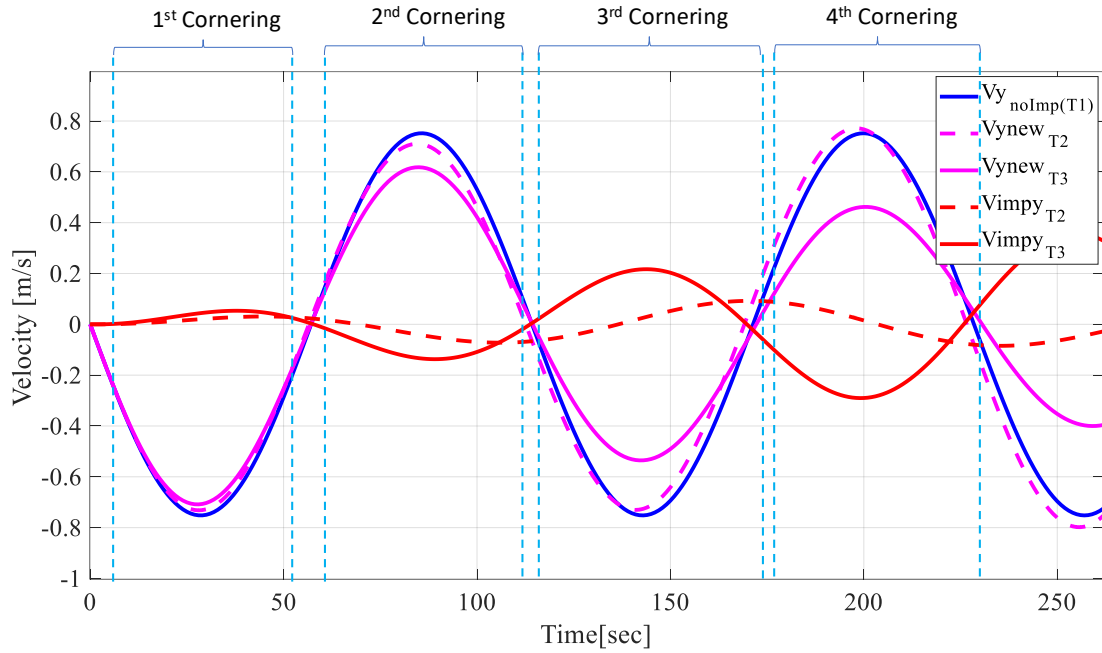**Fig. 9.** Sample of velocity input on X-axis MWV with and without impedance control

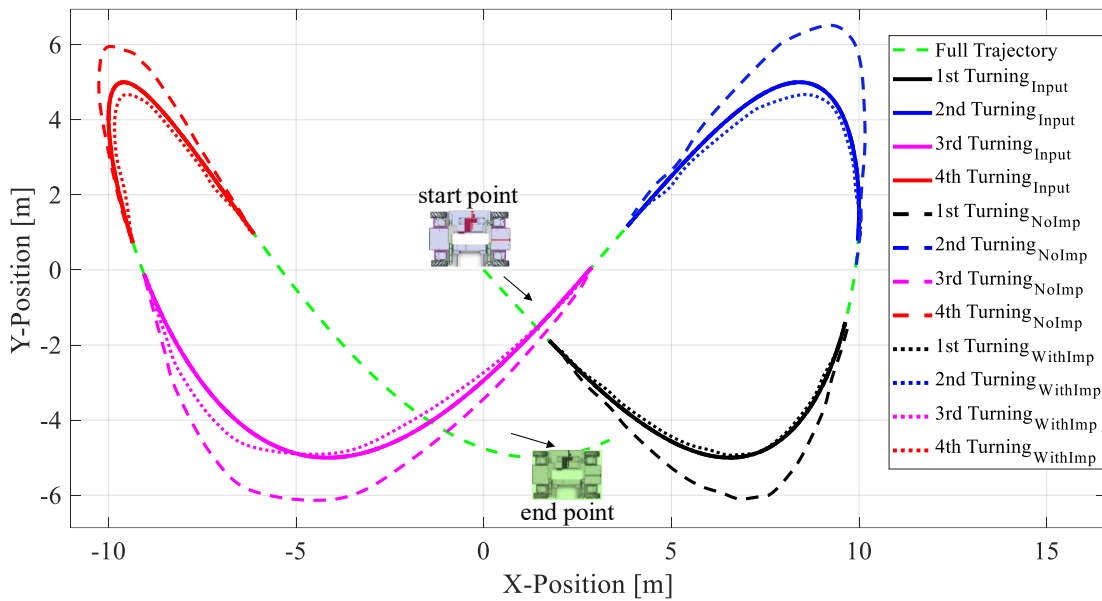**Fig. 10.** Sample of velocity input on *Y*-axis MWV with and without impedance control

Fig. 11. Sample of the X-Y path planning coordinate between a vehicle with and without impedance control

5. Conclusion

According to the overall results, the proposed control method is verified by providing inertia reduction and control by shaping the velocity input of the MWV through the regulation of each force axial of the vehicle itself. Concerning the overall performance, approximately 45% of kinetic energy can be reduced during the cornering motion of the vehicle by tuning stiffness and damping ratio values on each axial impedance control. With the proposed control, the vehicle gets slower during the cornering path, which correlates to the kinetic energy reduction. The proposed velocity-based impedance control has the potential to be optimized with some learning system, and this will become one of the future works in this study.
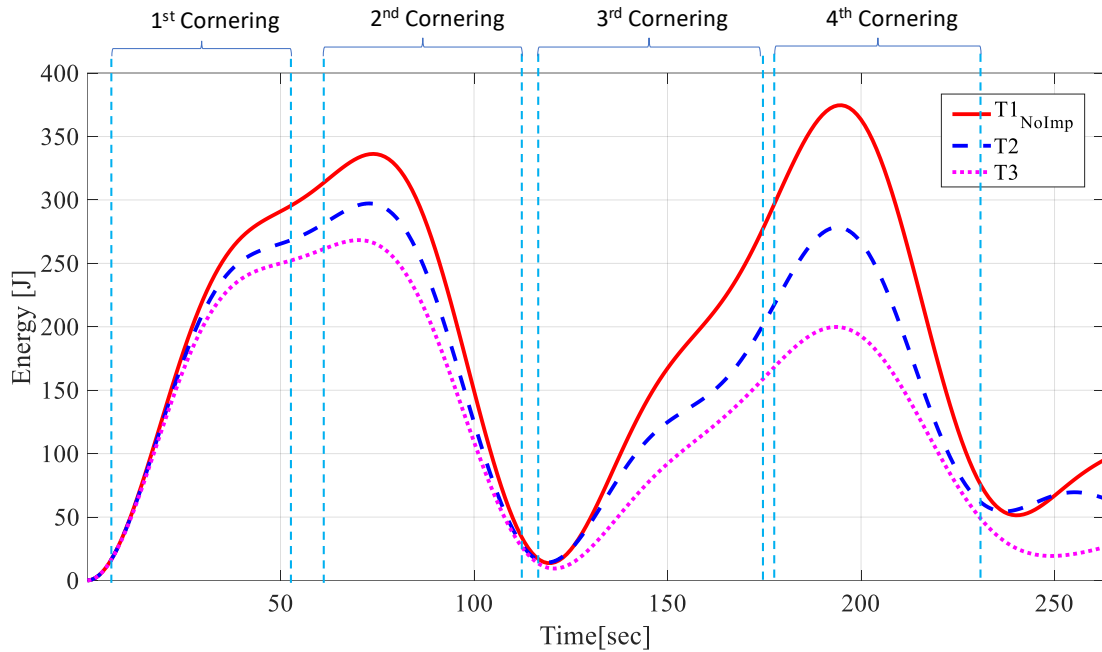
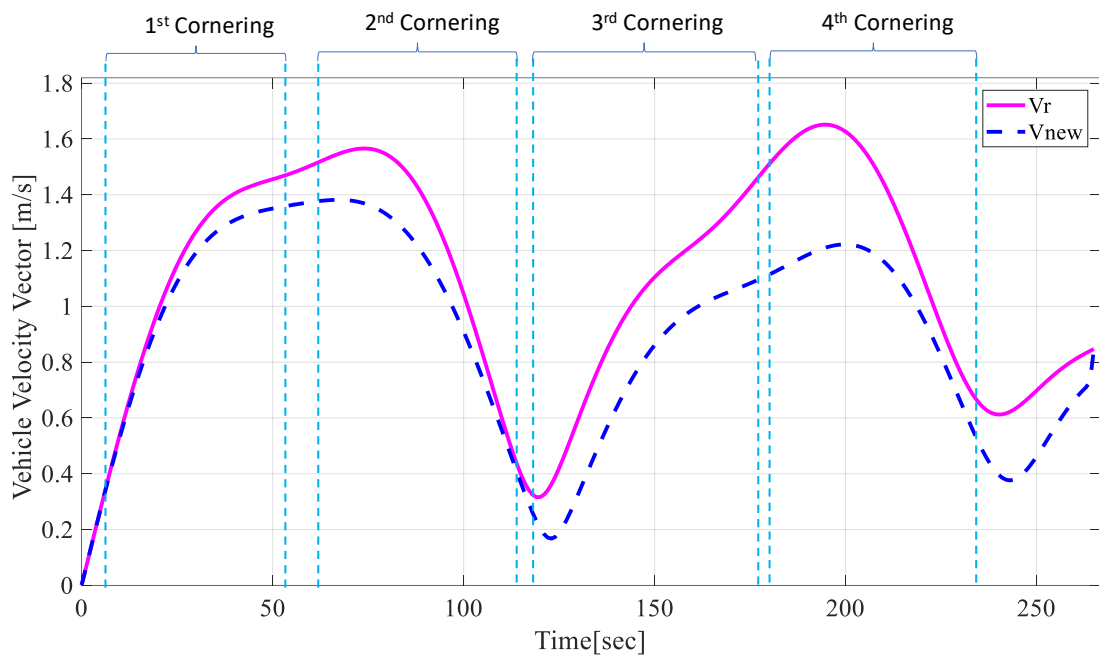**Fig. 12.** Kinetic energy performance of MWV for different simulation sessions

Fig. 13. Velocity input vector performances of MWV vehicle; with and without impedance control

References

[1] R. Siegwart and I. R. Nourbakhsh, *Introduction to Autonomous Mobile Robots*. MIT Press, 2004, https://books.google.co.id/books?id=gUbQ9_weg88C.

[2] P. I. T. Chang, C. C. Liu, S. C. F. Chiang, and C. Y. Lan, "Signal-based and Model-based Wheel Fault Detection of Omni-directional Vehicle with Mecanum Wheel," in *2020 International Automatic Control Conference (CACS)*, 2020, pp. 1-6, https://doi.org/10.1109/CACS50047.2020.9289703.

[3] A. S. Oo, M. Y. Naing, I. Nilkhamhang, and T. Than, "Experiment on Real-Time Image Processing in the Controlling of Mecanum Wheel Robotic Car," in *2019 First International Symposium on Instrumentation, Control, Artificial Intelligence, and Robotics (ICA-SYMP)*, 2019, pp. 41-44, https://doi.org/10.1109/ICA-SYMP.2019.8646199.

[4] N. M. Adam, A. Irawan, and M. A. Ahmad, "Robust super-twisting sliding mode controller for the lateral and longitudinal dynamics of rack steering vehicle," *Bulletin of Electrical Engineering and Informatics,* vol. 11, pp. 1882-1891, 2022, https://doi.org/10.11591/eei.v11i4.3641.

[5] Y. Jiang, H. Meng, G. Chen, C. Yang, X. Xu, L. Zhang, and H. Xu, "Differential-steering based path tracking control and energy-saving torque distribution strategy of 6WID unmanned ground vehicle," *Energy,* vol. 254, p. 124209, 2022, https://doi.org/10.1016/j.energy.2022.124209.

[6] G. Bayar and S. Ozturk, "Investigation of The Effects of Contact Forces Acting on Rollers Of a Mecanum Wheeled Robot," *Mechatronics,* vol. 72, p. 102467, 2020, https://doi.org/10.1016/j.mechatronics.2020.102467.

[7] Z. Yu, X. Huang, and J. Wang, "A least-squares regression based method for vehicle yaw moment of inertia estimation," in *2015 American Control Conference (ACC)*, 2015, pp. 5432-5437, https://doi.org/10.1109/ACC.2015.7172189.

[8] C. L. Qian, S Lee, C Ma, "Robust formation maneuvers through sliding mode for multi-agent systems with uncertainties," *IEEE/CAA Journal of Automatica Sinica,* vol. 5, pp. 342-351, 2018, https://doi.org/10.1109/JAS.2017.7510787.

[9] D. Nemec, V. Šimák, A. Janota, M. Hruboš, and E. Bubeníková, "Precise localization of the mobile wheeled robot using sensor fusion of odometry, visual artificial landmarks and inertial sensors," *Robotics and Autonomous Systems,* vol. 112, pp. 168-177, 2019, https://doi.org/10.1016/j.robot.2018.11.019.

[10] A. Irawan, M. A. Yaacob, F. A. Azman, M. R. Daud, A. R. Razali, and S. N. S. Ali, "Vision-based Alignment Control for Mini Forklift System in Confine Area Operation," in *2018 International Symposium on Agent, Multi-Agent Systems and Robotics (ISAMSR)*, 2018, pp. 1-6, https://doi.org/10.1109/ISAMSR.2018.8540552.

[11] R. H. Ali Faris, A. A. Ibrahim, N. B. Mohamad wasel, M. M. Abdulwahid, and M. F. Mosleh, "Optimization and Enhancement of Charging Control System of Electric Vehicle Using MATLAB SIMULINK," *IOP Conference Series: Materials Science and Engineering,* vol. 1105, p. 012004, 2021, https://doi.org/10.1088/1757-899X/1105/1/012004.

[12] J. Fu and R. C. Hill, "Development of a Multi-Stage Control Strategy for Omnidirectional Mobility in the Presence of Slip," in *2018 IEEE 61st International Midwest Symposium on Circuits and Systems (MWSCAS)*, 2018, pp. 376-379, https://doi.org/10.1109/MWSCAS.2018.8624090.

[13] M. Cui, H. Liu, W. Liu, and Y. Qin, "An Adaptive Unscented Kalman Filter-based Controller for Simultaneous Obstacle Avoidance and Tracking of Wheeled Mobile Robots with Unknown Slipping Parameters," *Journal of Intelligent & Robotic Systems,* vol. 92, pp. 489-504, 2018, https://doi.org/10.1007/s10846-017-0761-9.

[14] V. Rajagopalan, M. Ç, and A. Kelly, "Slip-aware Model Predictive optimal control for Path following," in *2016 IEEE International Conference on Robotics and Automation (ICRA)*, 2016, pp. 4585-4590, https://doi.org/10.1109/ICRA.2016.7487659.

[15] X. Huang and J. Wang, "Real-Time Estimation of Center of Gravity Position for Lightweight Vehicles Using Combined AKF–EKF Method," *IEEE Transactions on Vehicular Technology,* vol. 63, pp. 4221-4231, 2014, https://doi.org/10.1109/TVT.2014.2312195.

[16] H. Xiao, Z. Li, C. Yang, L. Zhang, P. Yuan, L. Ding, and T. Wang, "Robust Stabilization of a Wheeled Mobile Robot Using Model Predictive Control Based on Neurodynamics Optimization," *IEEE Transactions on Industrial Electronics,* vol. 64, pp. 505-516, 2017, https://doi.org/10.1109/TIE.2016.2606358.

[17] F. C. R. Pinheiro, M. R. O. d. A. Máximo, and T. Yoneyama, "Model Predictive Control for Omnidirectional Small Size Robot with Motor and Non-Slipping Constraints," in *2019 Latin American Robotics Symposium (LARS), 2019 Brazilian Symposium on Robotics (SBR) and 2019 Workshop on Robotics in Education (WRE)*, 2019, pp. 13-18, https://doi.org/10.1109/LARS-SBR-WRE48964.2019.00011.

[18] M. Deremetz, R. Lenain, B. Thuilot, and V. Rousseau, "Adaptive trajectory control of off-road mobile robots: A multi-model observer approach," in *2017 IEEE International Conference on Robotics and Automation (ICRA)*, 2017, pp. 4407-4413, https://doi.org/10.1109/ICRA.2017.7989509.

[19] B. I. Adamov and G. R. Saypulaev, "A Study of the Dynamics of an Omnidirectional Platform, Taking into Account the Design of Mecanum Wheels and Multicomponent Contact Friction," in *2020 International Conference Nonlinearity, Information and Robotics (NIR)*, 2020, pp. 1-6, https://doi.org/10.1109/NIR50484.2020.9290193.

[20] B. Seo, "Path Following Control for Military Automobiles using Dynamic Inversion Method," in *2019 International Conference on Information and Communication Technology Convergence (ICTC)*, 2019, pp. 617-622, https://doi.org/10.1109/ICTC46691.2019.8939869.

[21] S. Cheng, L. Li, C. -Z. Liu, X. Wu, S. -N. Fang, and J. Yong, "Robust LMI-Based H-Infinite Controller Integrating AFS and DYC of Autonomous Vehicles With Parametric Uncertainties," *IEEE Transactions on Systems, Man, and Cybernetics: Systems*, vol. 51, no. 11, pp. 6901-6910, Nov. 2021, https://doi.org/10.1109/TSMC.2020.2964282.

[22] C. Katrakazas, M. Quddus, W.-H. Chen, and L. Deka, "Real-time motion planning methods for autonomous on-road driving: State-of-the-art and future research directions," *Transportation Research Part C: Emerging Technologies,* vol. 60, pp. 416-442, 2015, https://doi.org/10.1016/j.trc.2015.09.011.

[23] N. M. Adam and A. Irawan, "Modeling and Analysis of Omnidirectional Wheeled Vehicles Using Velocity-Based Impedance Control," in *Enabling Industry 4.0 through Advances in Mechatronics*, Singapore, 2022, pp. 485-495, https://doi.org/10.1007/978-981-19-2095-0_41.

[24] F. K. Faudzi and A. Irawan, "Steering Angle Control of Rack Steering Vehicle using Antiwindup-PI-Control," *International Journal of Electrical Engineering and Applied Sciences (IJEEAS),* vol. 3, pp. 61-66, 2020, https://ijeeas.utem.edu.my/ijeeas/article/view/5821.

[25] C. b. Moon and W. Chung, "Kinodynamic Planner Dual-Tree RRT (DT-RRT) for Two-Wheeled Mobile Robots Using the Rapidly Exploring Random Tree," *IEEE Transactions on Industrial Electronics,* vol. 62, pp. 1080-1090, 2015, https://doi.org/10.1109/TIE.2014.2345351.

[26] F. Xiao, "Optimal torque distribution for four-wheel-motored electric vehicle stability enhancement," in *2015 IEEE International Transportation Electrification Conference (ITEC)*, 2015, pp. 1-9, https://doi.org/10.1109/ITEC-India.2015.7386885.

[27] Z. Shenghao and S. Jinchun, "Impedance Control for Vehicle Driving with Human Operation Under Unstructured Environment," in *2011 International Conference on Internet Computing and Information Services*, 2011, pp. 159-162, https://doi.org/10.1109/ICICIS.2011.46.

[28] T. Enmei, H. Fujimoto, and Y. Hori, "Proposal of impedance control for electric vehicles with wheel resolver - application to hand assisted parking and position adjustment," in *IECON 2016 - 42nd Annual Conference of the IEEE Industrial Electronics Society*, 2016, pp. 6435-6440, https://doi.org/10.1109/IECON.2016.7793970.

[29] Y. W. Jeong, C. C. Chung, and W. Kim, "Nonlinear Hybrid Impedance Control for Steering Control of Rack-Mounted Electric Power Steering in Autonomous Vehicles," *IEEE Transactions on Intelligent Transportation Systems,* vol. 21, pp. 2956-2965, 2020, https://doi.org/10.1109/TITS.2019.2921893.

[30] A. Irawan, M. I. P. Azahar, and Z. H. Ismail, "Interaction Motion on Pneumatic Cylinder using Prescribed Performance Force Tracking Impedance Control," in *2020 8th International Conference on Control, Mechatronics and Automation (ICCMA)*, 2020, pp. 121-126, https://doi.org/10.1109/ICCMA51325.2020.9301501.

[31] C. Yao, M. Schuster, Z. Jiang, K. Janschek, and M. Beitelschmidt, "Sensitivity Analysis of Model-based Impedance Control for Physically Interactive Hexarotor," *IFAC-PapersOnLine,* vol. 52, pp. 597-602, 2019, https://doi.org/10.1016/j.ifacol.2019.11.741.

[32] B. Komati, C. Clevy, and P. Lutz, "Force tracking impedance control with unknown environment at the microscale," in *2014 IEEE International Conference on Robotics and Automation (ICRA)*, 2014, pp. 5203-5208, https://doi.org/10.1109/ICRA.2014.6907623.

[33] Y. Soh Chin, S. Parasuraman, and V. Ganapathy, "Dynamic Path Planning Algorithm In Mobile Robot Navigation," in *2011 IEEE Symposium on Industrial Electronics and Applications (ISIEA)*, 2011, pp. 364-369, https://doi.org/10.1109/ISIEA.2011.6108732.

[34] M. C. Koval, J. E. King, N. S. Pollard, and S. S. Srinivasa, "Robust trajectory selection for rearrangement planning as a multi-armed bandit problem," in *2015 IEEE/RSJ International Conference on Intelligent Robots and Systems (IROS)*, 2015, pp. 2678-2685, https://doi.org/10.1109/IROS.2015.7353743.

[35] A. Sintov and A. Shapiro, "A stochastic dynamic motion planning algorithm for object-throwing," in *2015 IEEE International Conference on Robotics and Automation (ICRA)*, 2015, pp. 2475-2480, https://doi.org/10.1109/ICRA.2015.7139530.

[36] S. Spanogianopoulos and K. Sirlantzis, "Non-holonomic path planning of car-like robot using RRT*FN," in *2015 12th International Conference on Ubiquitous Robots and Ambient Intelligence (URAI)*, 2015, pp. 53-57, https://doi.org/10.1109/URAI.2015.7358927.

[37] C. Xie, J. van den Berg, S. Patil, and P. Abbeel, "Toward asymptotically optimal motion planning for kinodynamic systems using a two-point boundary value problem solver," in *2015 IEEE International Conference on Robotics and Automation (ICRA)*, 2015, pp. 4187-4194, https://doi.org/10.1109/ICRA.2015.7139776.

[38] Z. Liu, X. Yuan, and Z. Li, "3-D path planning system for autonomous vehicle considering the rollover and path length," *Journal of the Franklin Institute,* vol. 359, pp. 5272-5287, 2022, https://doi.org/10.1016/j.jfranklin.2022.05.040.

[39] N. M. Adam, A. Irawan, M. R. Daud, Z. M. Zain, and S. N. S. Ali, "Dynamic modeling and analysis of omnidirectional wheeled robot: Turning motion analysis," *Journal of Telecommunication, Electronic and Computer Engineering,* vol. 10, pp. 103-108, 2018, https://core.ac.uk/download/pdf/229276002.pdf.

[40] M. M. Alam, A. Irawan, and T. Y. Yin, "Buoyancy effect control in multi legged robot locomotion on seabed using integrated impedance-fuzzy logic approach," *Indian Journal of Geo-marine Science*, vol. 44, pp. 1937-1945, 2015, http://nopr.niscpr.res.in/bitstream/123456789/34945/1/IJMS%2044%2812%29%201937-1945.pdf.